



# Validation of RWM Kinetic Stability Model and Physics Implications in NSTX

**J.W. Berkery, S.A. Sabbagh**

*Department of Applied Physics, Columbia University, New York, NY, USA*

**R. Betti, R.E. Bell, A. Diallo, S.P. Gerhardt, B.P. LeBlanc, J. Manickam, and M. Podestà**

*Princeton Plasma Physics Laboratory, Princeton, NJ, USA*

**Y.Q. Liu, I.T. Chapman**

*Euratom/CCFE Fusion Association, Culham Science Centre, Abingdon, OX14 3DB, UK*

**J.P. Graves**

*Ecole Polytechnique Federale de Lausanne (EPFL), Centre de Recherches en Physique des Plasmas, Association EURATOM-Confederation Suisse, 1015 Lausanne, Switzerland*

**Z.R. Wang**

*Consorzio RFX, Associazione EURATOM-ENEA sulla Fusione Corso Stati Uniti 4, 35127 Padova, Italy*

*College W&M  
 Colorado Sch Mines  
 Columbia U  
 CompX  
 General Atomics  
 INL  
 Johns Hopkins U  
 LANL  
 LLNL  
 Lonestar  
 MIT  
 Nova Photonics  
 New York U  
 Old Dominion U  
 ORNL  
 PPPL  
 PSI  
 Princeton U  
 Purdue U  
 SNL  
 Think Tank, Inc.  
 UC Davis  
 UC Irvine  
 UCLA  
 UCSD  
 U Colorado  
 U Illinois  
 U Maryland  
 U Rochester  
 U Washington  
 U Wisconsin*

*Culham Sci Ctr  
 U St. Andrews  
 York U  
 Chubu U  
 Fukui U  
 Hiroshima U  
 Hyogo U  
 Kyoto U  
 Kyushu U  
 Kyushu Tokai U  
 NIFS  
 Niigata U  
 U Tokyo  
 JAEA  
 Hebrew U  
 Ioffe Inst  
 RRC Kurchatov Inst  
 TRINITI  
 KBSI  
 KAIST  
 POSTECH  
 ASIPP  
 ENEA, Frascati  
 CEA, Cadarache  
 IPP, Jülich  
 IPP, Garching  
 ASCR, Czech Rep  
 U Quebec*

# Resistive wall mode stability can be explained by including kinetic effects ; Code calculations require benchmarking

- Motivation
  - Accurate calculation of the physics of RWM kinetic stabilization is key for disruption-free operation of a low collisionality burning plasma (ST-CTF, FNSF, ITER) at any rotation.
- Outline
  - Recent resonant field amplification and reduced internal inductance experimental results in NSTX are consistent with kinetic stability theory as calculated by the MISK code.
  - Kinetic stability calculations are being benchmarked through comparison with the results of other codes such as MARS-K and HAGIS. (ITPA MHD Stability group joint experiment MDC-2)
  - Corrected stability calculations improve agreement with experiments in cases tested to date.

# Kinetic terms in the RWM dispersion relation enable stabilization; theory consistent with experimental results

Dissipation ( $\text{Im}(\delta W_K)$ ) and restoring force ( $\text{Re}(\delta W_K)$ ) from kinetic term enables stabilization of the RWM:

$$(\gamma - i\omega_r) \tau_w = -\frac{\delta W_\infty + \delta W_K}{\delta W_b + \delta W_K}$$

[B. Hu *et al.*, Phys. Plasmas **12**, 057301 (2005)]

$$\delta W_K = \sum_j \sum_{l=-\infty}^{\infty} 2\sqrt{2}\pi^2 \int \int \int \left[ |\langle H/\hat{\varepsilon} \rangle|^2 \frac{(\omega - n\omega_E) \frac{\partial f_j}{\partial \varepsilon} - \frac{n}{Z_j e} \frac{\partial f_j}{\partial \Psi}}{n\langle \omega_D^j \rangle + l\omega_b^j - i\nu_{\text{eff}}^j + n\omega_E - \omega} \right] \frac{\hat{\tau}}{m_j^{\frac{3}{2}} B} |\chi|^{\hat{\varepsilon}^{\frac{5}{2}}} d\hat{\varepsilon} d\chi d\Psi, \quad \chi = v_{\parallel}/v$$



- MISK calculations are consistent with RWM instability at intermediate plasma rotation in NSTX
- Instability appears between precession drift resonance at low  $\omega_\phi$ , bounce/transit resonance at high  $\omega_\phi$

[S. Sabbagh *et al.*, Nucl. Fusion **50**, 025020 (2010)]

[J. Berkery *et al.*, Phys. Rev. Lett. **104**, 035003 (2010)]

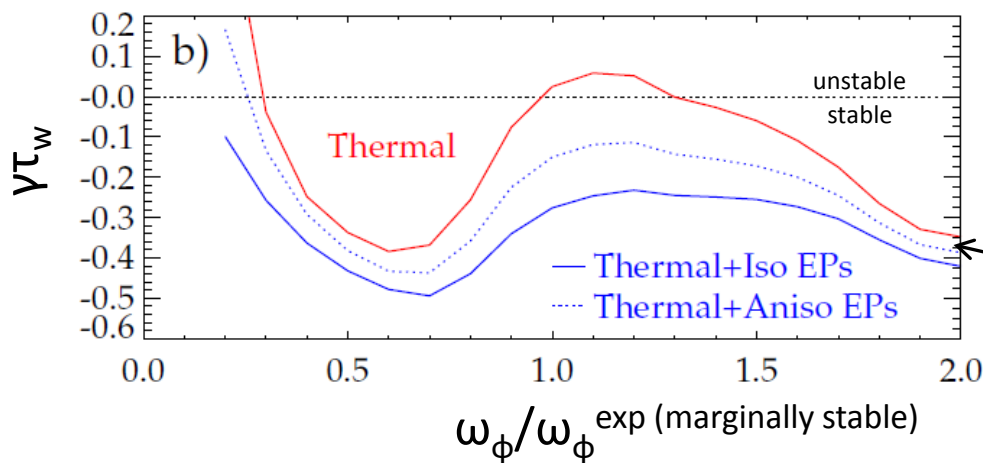
# Improving quantitative agreement: EPs are generally stabilizing; Anisotropic distribution impacts stability

$$\delta W_K \sim \left[ \frac{1}{\langle \omega_D \rangle + l\omega_b - i\nu_{\text{eff}} + \omega_E} \right]$$

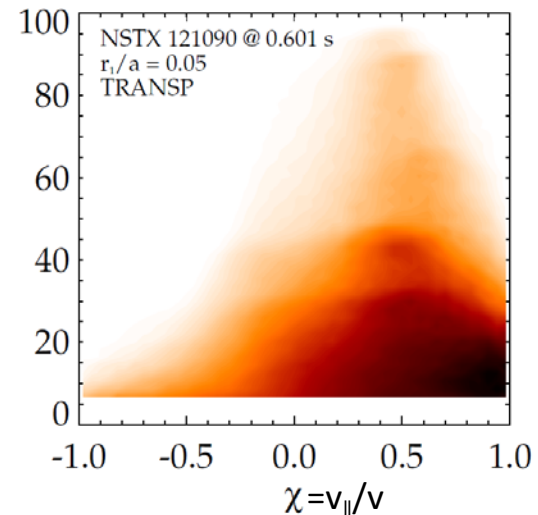
small for Energetic Particles (EPs)

- EPs provide stabilizing force that is nearly independent of  $\omega_\phi$
- EPs generally are not in mode resonance, so the effect is not energy dissipation, but rather a restoring force

[J.W. Berkery *et al.*, Phys. Plasmas **17**, 082504 (2010)]



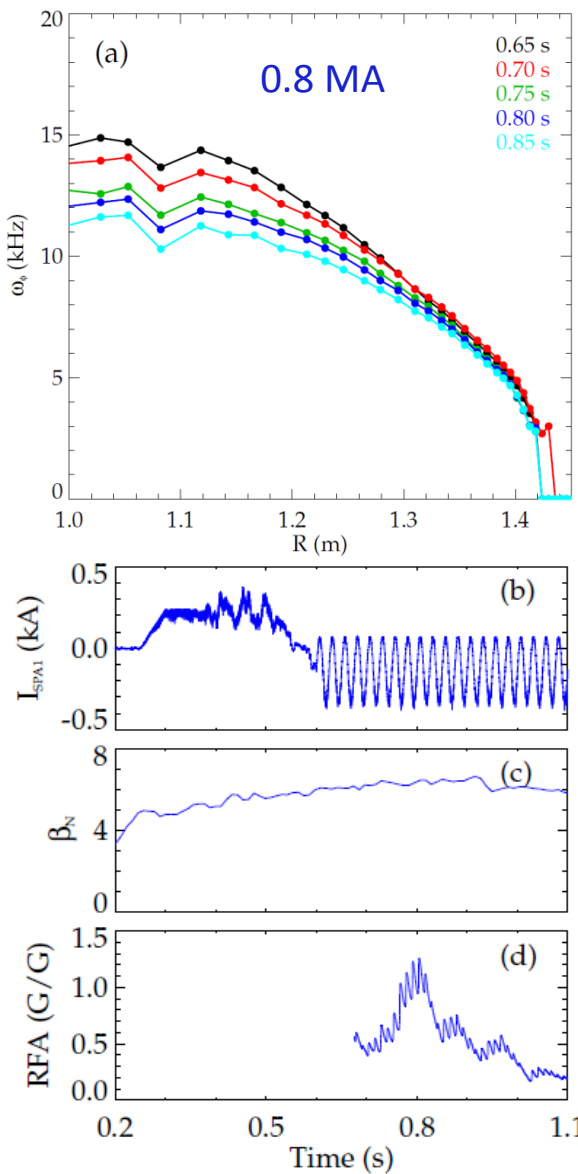
Beam ions are anisotropic



$$f(\varepsilon, \Psi, \chi) = \frac{C(\Psi)}{\varepsilon^{\frac{3}{2}} + \varepsilon_c^{\frac{3}{2}}} \frac{e^{-(\chi - \chi_0)^2 / \delta \chi^2}}{\delta \chi}$$

Addition of simple anisotropy model ( $\chi_0 = 0.75$ ,  $\delta\chi = 0.25$ ) reduces stabilizing effect, consistent with quantitative comparison to NSTX plasmas

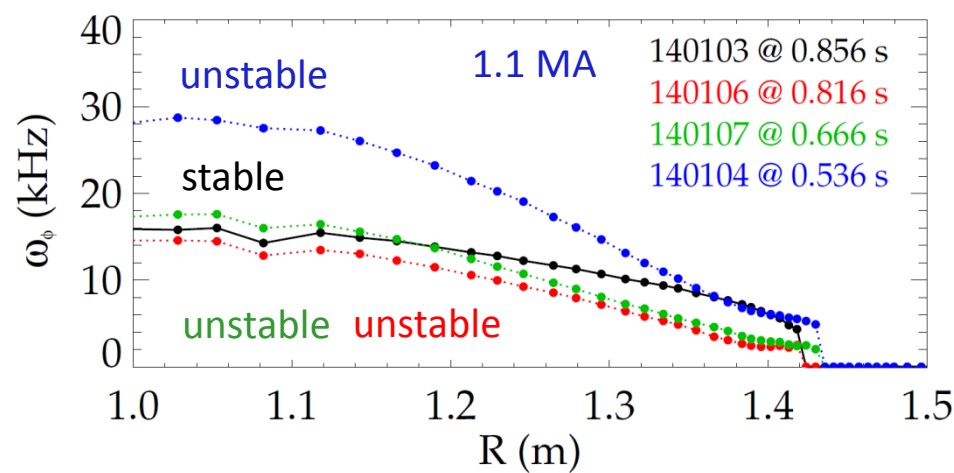
# An NSTX experiment explored RWM stability with $\omega_\phi$ and EP fraction, with RFA measurements, for comparison to kinetic theory



Resonant field amplification (RFA) amplitude is a measure of RWM stability.

$$RFA = \frac{B_{plasma}}{B_{applied}}$$

- $\omega_\phi$  slowed with  $n=3$  magnetic braking for various EP fractions ( $I_p$ ,  $B_t$  scan)
  - Weak stability region at intermediate  $\omega_\phi$  shows in RFA
  - Plasma can survive it (left), or not (below).
  - Kinetic analysis with MISK was performed.
  - Many shots with long, slow, rotation decreases and many RFA periods were obtained.

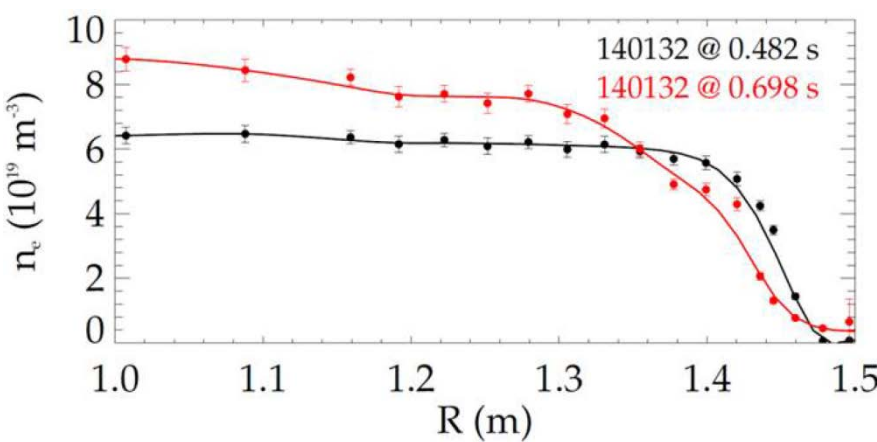


# Kinetic stability calculations show reduced stability in low $I_i$ target plasma as $\omega_\phi$ is reduced, RWM becomes unstable

- Stability evolves

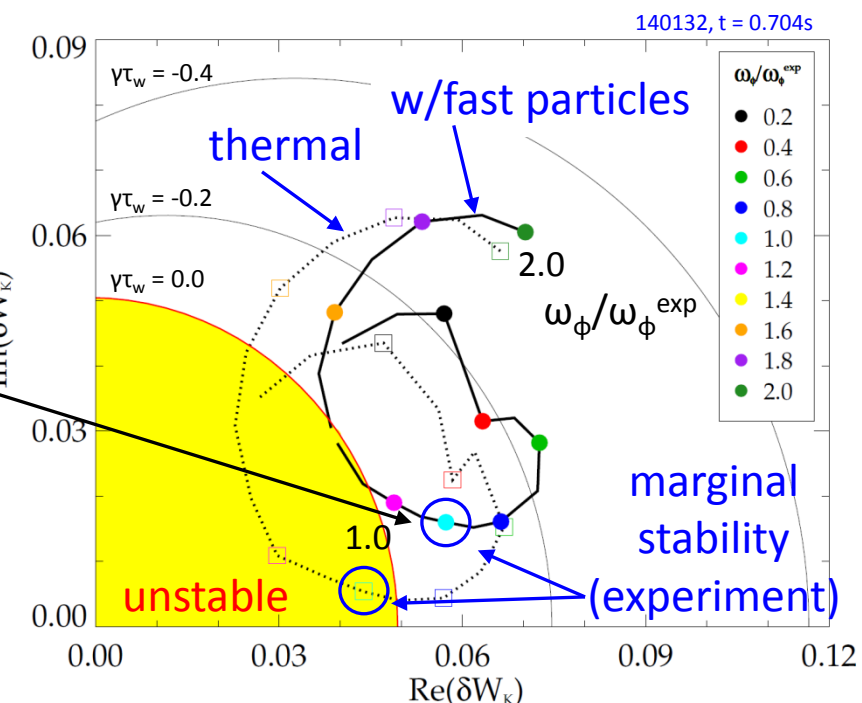
MISK code

- MISK computation shows plasma to be stable at time of minimum  $I_i$
- Region of reduced stability vs.  $\omega_\phi$  found before RWM becomes unstable ( $I_i = 0.49$ )
  - Co-incident with a drop in edge density gradient – reduces kinetic stabilization



[S.A. Sabbagh *et al.*, APS Invited 2010 paper GI2.01]

RWM stability vs.  $\omega_\phi$  (contours of  $\gamma\tau_w$ )

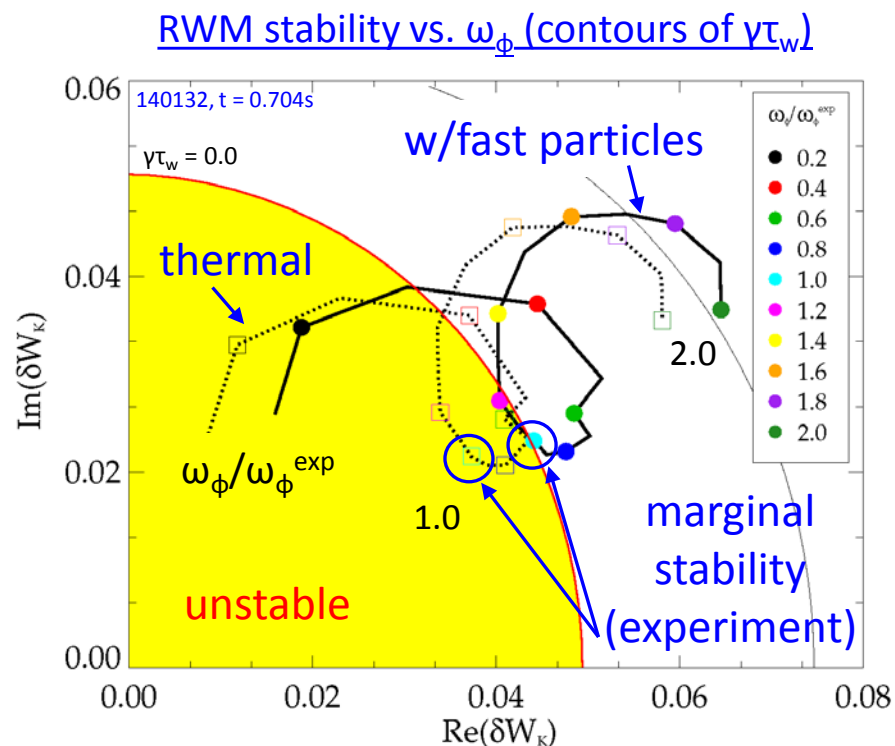


- Directly testing the RWM stability calculation at the marginal point in this NSTX experimentally unstable plasma.
- This past calculation showed close, but not full, quantitative agreement.
  - Investigating what might lead to improvement...

# Kinetic stability calculations are improved by additional physics and code development

- Additional physics (EPs) improves model, but doesn't bring full agreement
  - Also improves understanding of differences between devices (see: [S. Sabbagh *et al.*, IAEA FES 2010, Paper EXS/5-5], [H. Reimerdes *et al.*, Phys. Rev. Lett. **106**, 215002 (2011)])
- Correction to  $\omega_D$  from MDC-2 benchmarking further improves agreement (benchmarking investigation results later in the talk...)

## Corrected $\omega_D$



# MDC-2 Benchmarking of kinetic models: overview & steps

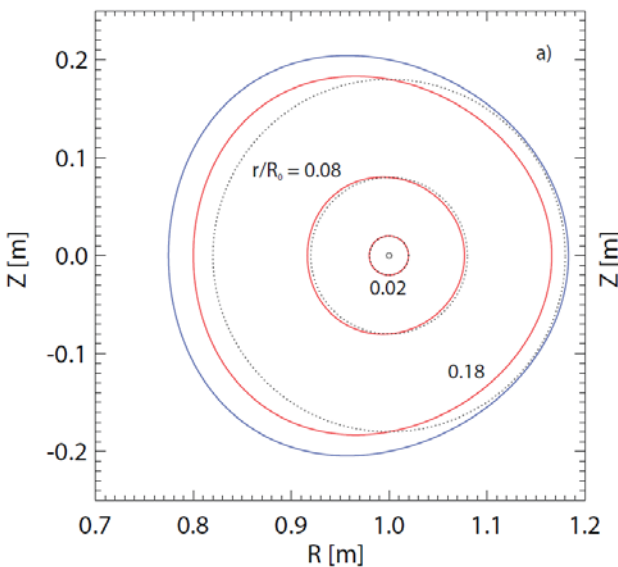
- Codes: HAGIS, MARS-K, MISK
- Choice of equilibria for benchmarking
  - Start by using Solov'ev
    - HAGIS / MARS-K, and MISK / MARS-K benchmarked to different degrees using Solov'ev equilibria; collect/cross compare results
      - HAGIS/MARS results published [Y. Liu et al., Phys. Plasmas **15**, 112503 (2008)]
      - Simplicity may lead to unrealistic anomalies – better to use realistic cases?
  - Move on to ITER-relevant equilibria
    - Use Scenario IV, or new equilibria recently generated for WG7 task by Y. Liu (more realistic; directly applicable to ITER)
    - Need kinetic profiles as well as fluid pressure
- Approach to stability comparison – start with
  - ideal fluid quantities ( $\delta W^{\text{no-wall}}$ ,  $\delta W^{\text{wall}}$ , etc.)
  - $n = 1$  (consider  $n > 1$  in a future step)
  - perturbative approach on static eigenfunction input - ensure that unstable eigenfunction is consistent among codes (e.g. no-wall ideal for MISHKA)
  - no-wall / with-wall  $\beta_N$  limits (equilibrium  $\beta$  scan needed)

Spring 2011

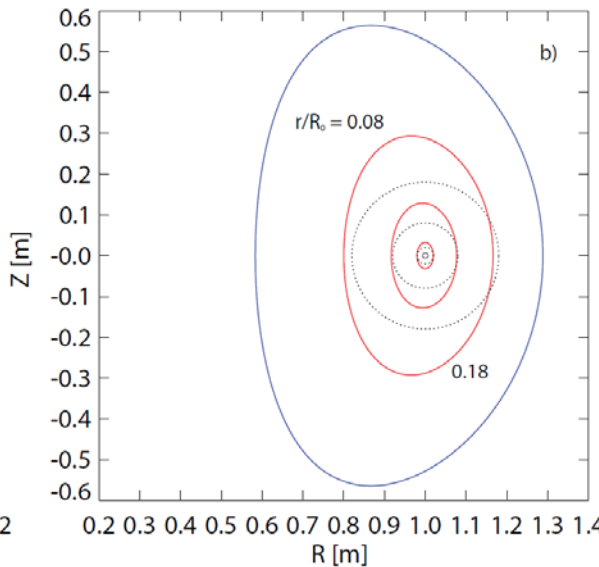
Fall 2011

# Started code comparison with simple equilibria and profile assumptions

Solov'ev case 1 (near-circular)



Solov'ev case 3 (shaped)



$$\mu_0 P(\psi) = -\frac{1 + \kappa^2}{\kappa R_0^3 q_0} \psi, \quad F(\psi) = 1$$

$$\psi = \frac{\kappa}{2R_0^3 q_0} \left[ \frac{R^2 Z^2}{\kappa^2} + \frac{1}{4} (R^2 - R_0^2)^2 - a^2 R_0^2 \right]$$

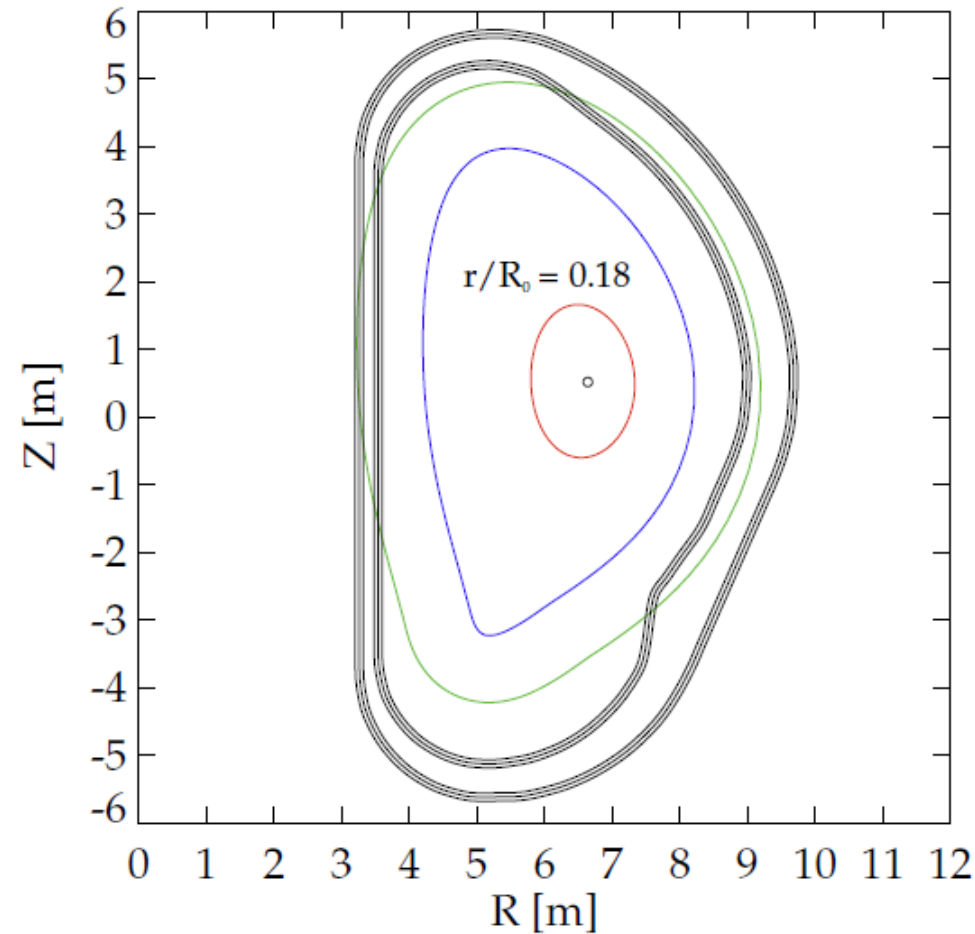
$$\delta W_K \propto \int \left[ \frac{\omega_{*N} + \left(\hat{\varepsilon} - \frac{3}{2}\right) \omega_{*T} + \omega_E}{\langle \omega_D \rangle + l\omega_b + \omega_E} \right] \hat{\varepsilon}^{\frac{5}{2}} e^{-\hat{\varepsilon}} d\hat{\varepsilon}$$

Simplified resonant denominator due to assumptions

- Common ground for codes (MARS / HAGIS / MISK)
  - Solov'ev equilibria
  - Codes run in perturbative mode
  - Density gradient constant
  - No energetic particles
  - $\omega_r, \gamma, v_{\text{eff}} = 0$

# Expanded comparison to include ITER equilibrium

- More realistic case (ITER)
  - ITPA MHD WG7 equilibrium
    - $I_p = 9 \text{ MA}$ ,  $\beta_N = 2.9$  (7% above  $n = 1$  no-wall limit)
  - Codes run in perturbative mode
  - With/without energetic particles
  - $\omega_r, \gamma, v_{\text{eff}} = 0$

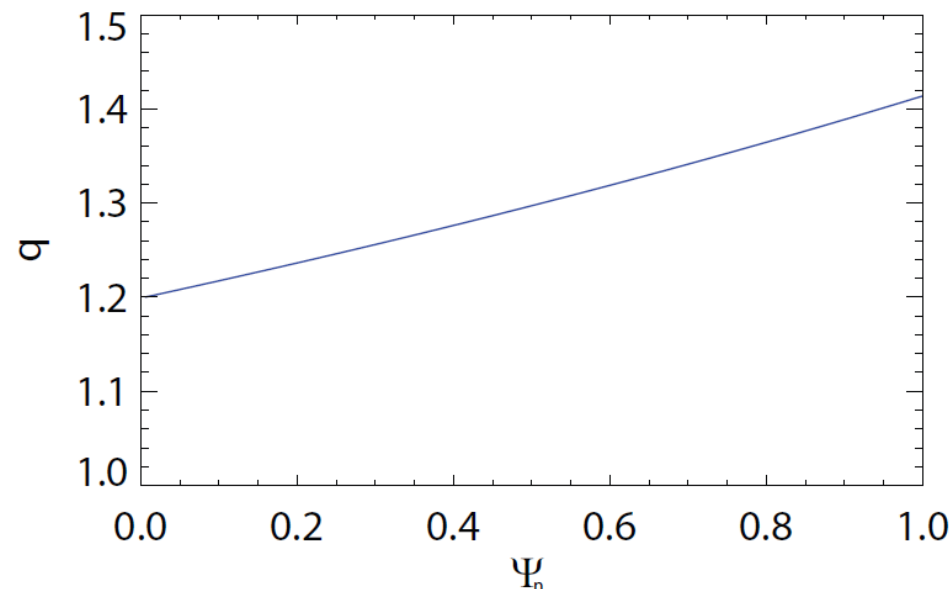


$$\delta W_K \propto \int \left[ \frac{\omega_{*N} + \left( \hat{\varepsilon} - \frac{3}{2} \right) \omega_{*T} + \omega_E}{\langle \omega_D \rangle + l\omega_b + \omega_E} \right] \hat{\varepsilon}^{\frac{5}{2}} e^{-\hat{\varepsilon}} d\hat{\varepsilon}$$

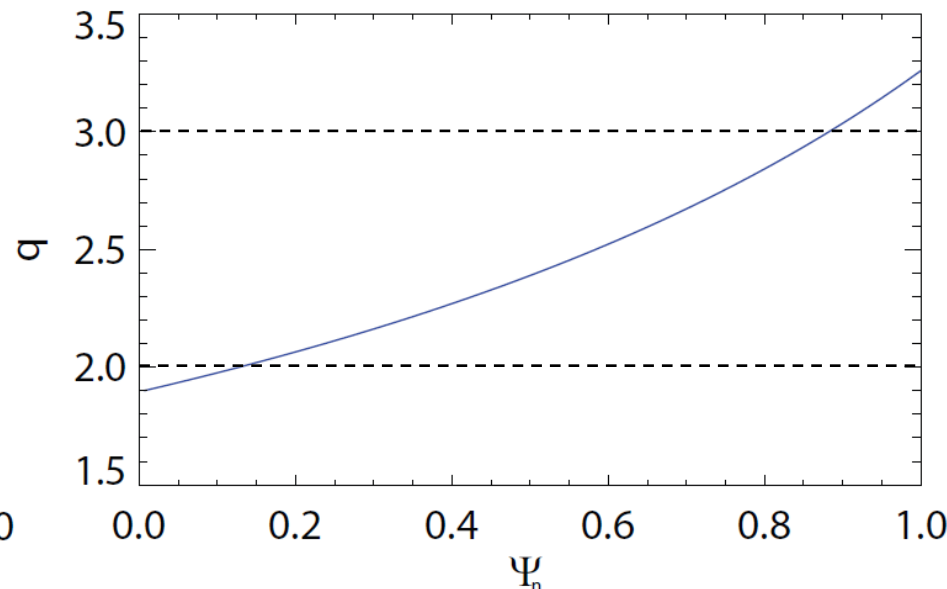
Note: Simplified resonant denominator due to assumptions

# Shaped vs. near-circular Solov'ev cases have important q profile differences for benchmarking

Solov'ev case 1 (near-circular)



Solov'ev case 3 (shaped)

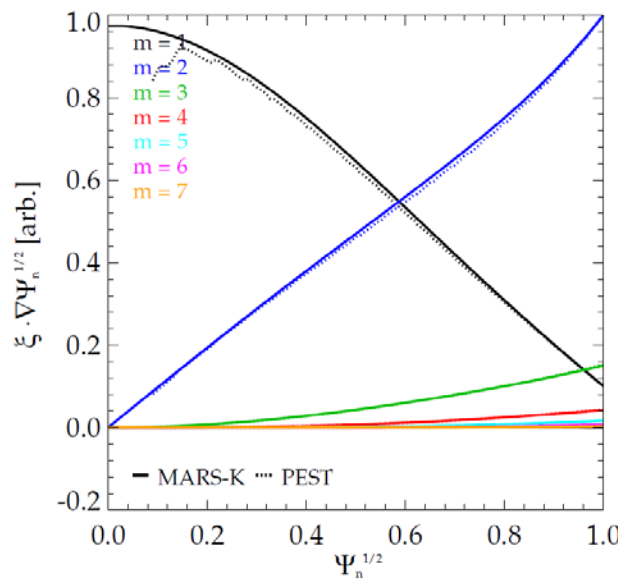


- No  $n = 1$  rational surfaces
  - Eliminates potential differences between calculation of kinetic dissipation at rational surfaces
- ITER equilibrium: rev. shear,  $q_0 \sim 2.2$ ,  $q_{\min} \sim 1.7$ ,  $q_a \sim 7.1$

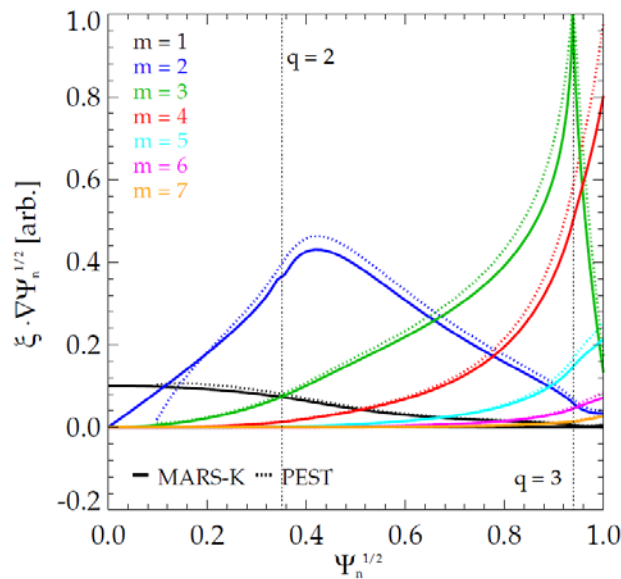
Differences in how MARS, MISK, HAGIS consider mode dissipation at rational surfaces is thought to be key – will be a main focus of next steps

# Eigenfunction benchmarking calculations were made to yield similar eigenfunctions, which are verified

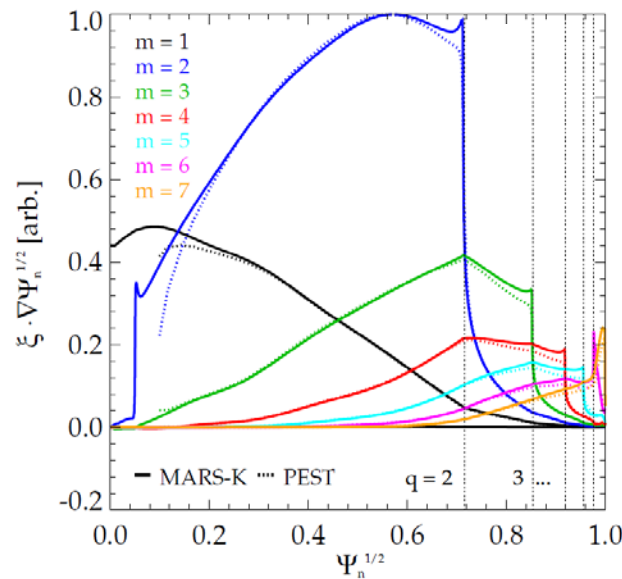
Solov'ev case 1 (near-circular)



Solov'ev case 3 (shaped)



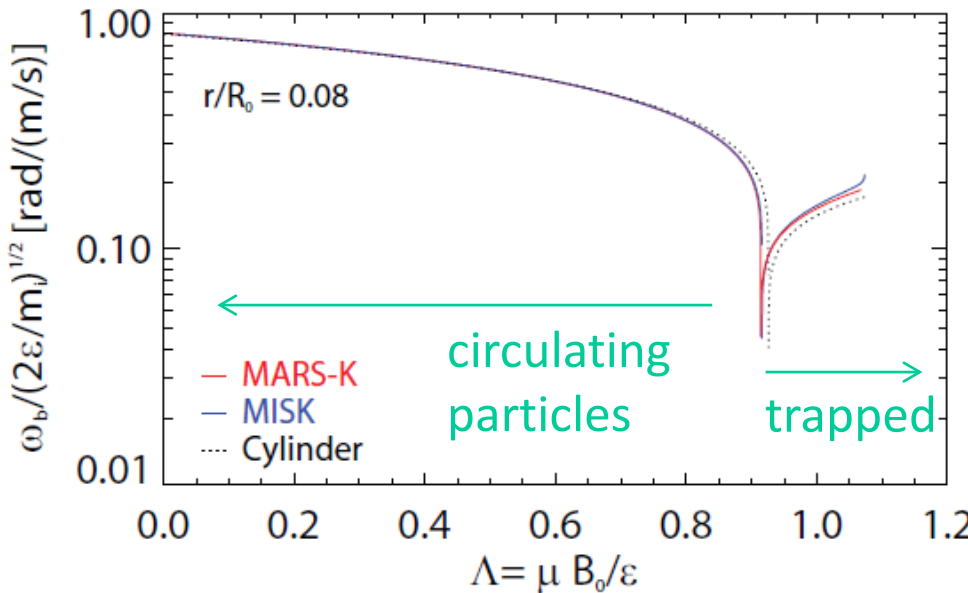
ITER



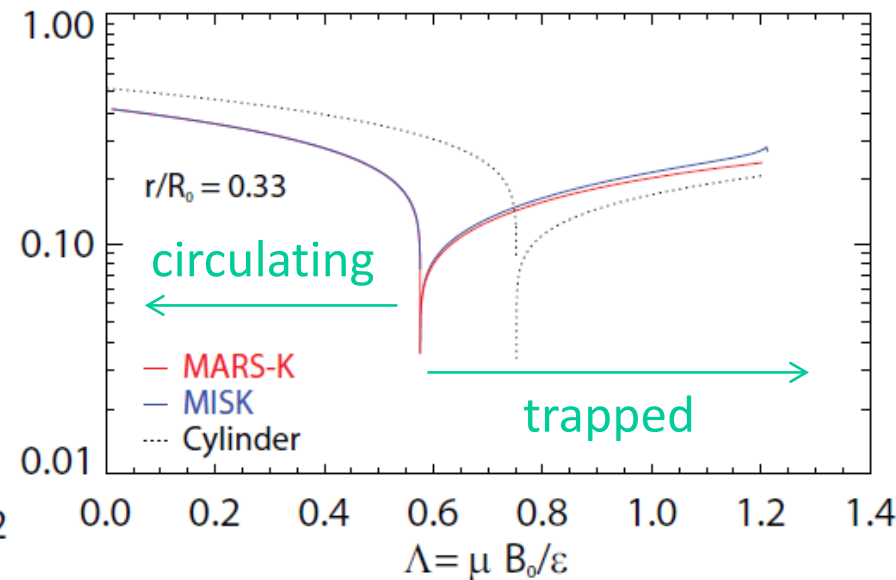
- PEST, MARS-K compared with-wall RWM
  - In PEST we use the wall position that yields marginal stability
  - PEST, MARS-K, and MISHKA compared for no-wall ideal kink
- There are some differences at rational surfaces
  - May lead to stability differences between MISK and MARS calculations

# Bounce frequency vs. pitch angle compares well between codes

Solov'ev case 1 (near-circular)



Solov'ev case 3 (shaped)



$$\frac{\omega_b}{\sqrt{2\epsilon/m_i}} = \frac{\sqrt{2\epsilon_r \Lambda B_0}}{4qR_0} \frac{\pi}{K(k)} \quad (\text{trapped})$$

$$k = \left[ \frac{1 - \Lambda B_0 + \epsilon_r \Lambda B_0}{2\epsilon_r \Lambda B_0} \right]^{\frac{1}{2}}$$

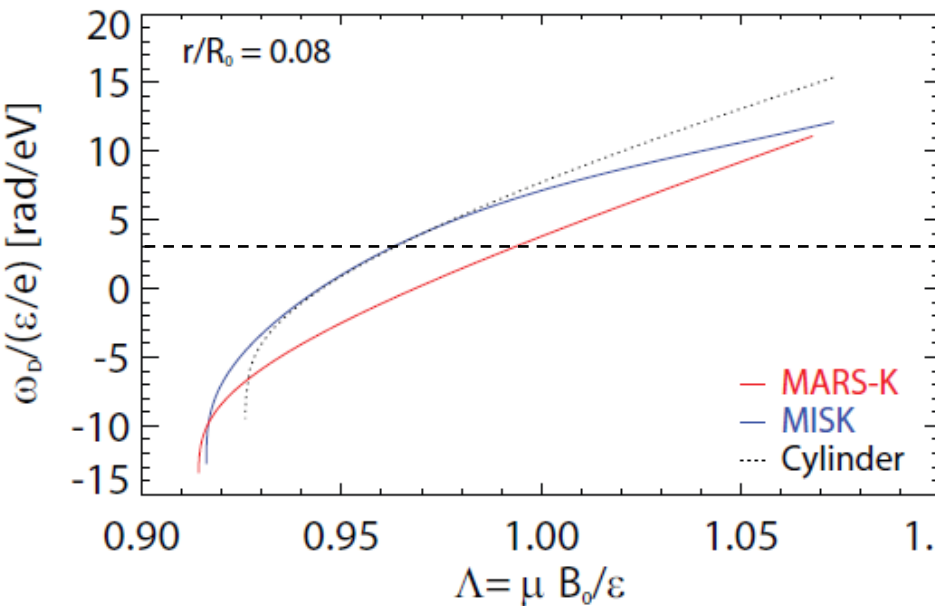
$$\frac{\omega_b}{\sqrt{2\epsilon/m_i}} = \frac{\sqrt{1 - \Lambda B_0 + \epsilon_r \Lambda B_0}}{2qR_0} \frac{\pi}{K(1/k)} \quad (\text{circulating})$$

large aspect ratio approximation

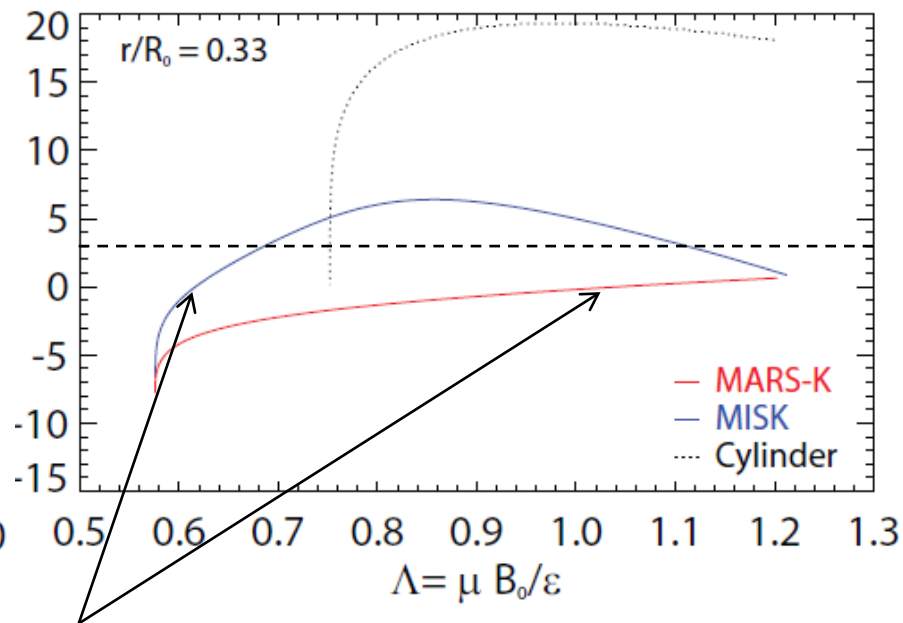
here,  $\epsilon_r$  is the inverse aspect ratio,  $s$  is the magnetic shear,  $K$  and  $E$  are the complete elliptic integrals of the first and second kind, and  $\Lambda = \mu B_0/\epsilon$ , where  $\mu$  is the magnetic moment and  $\epsilon$  is the kinetic energy.

# Significant issue found: precession drift frequencies did not agree

Solov'ev case 1 (near-circular)



Solov'ev case 3 (shaped)



- Clear difference in drift reversal point, even in near-circular case
- Issue found and corrected: metric coefficients for non-orthogonal grid incorrect in PEST interface to MISK

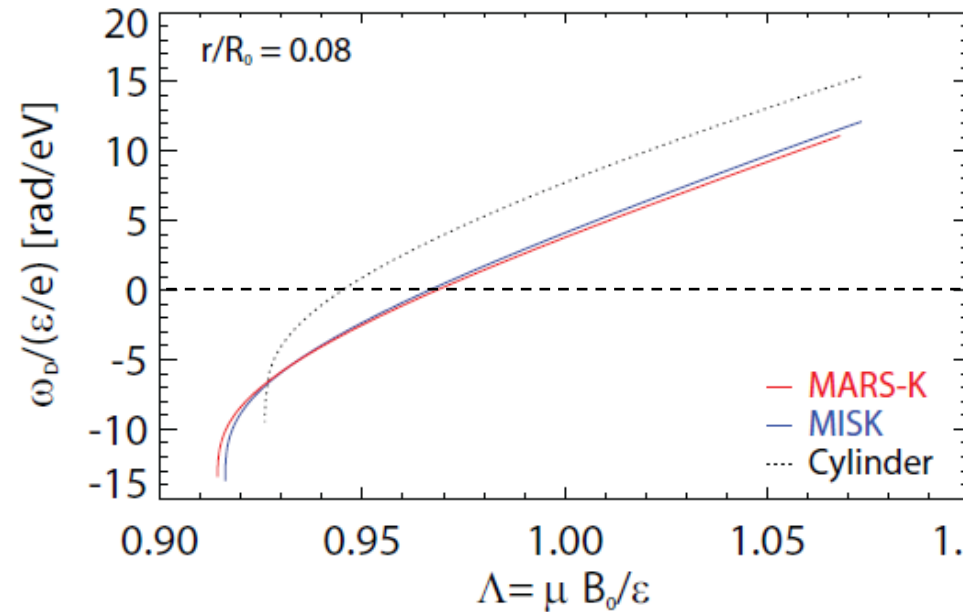
large aspect ratio approximation

$$\frac{\langle \omega_D \rangle}{\varepsilon/e} = \frac{2q\Lambda}{R_0^2 B_0 \epsilon_r} \left[ (2s+1) \frac{E(k^2)}{K(k^2)} + 2s(k^2 - 1) - \frac{1}{2} \right] \quad k = \left[ \frac{1 - \Lambda + \epsilon_r \Lambda}{2\epsilon_r \Lambda} \right]^{\frac{1}{2}}$$

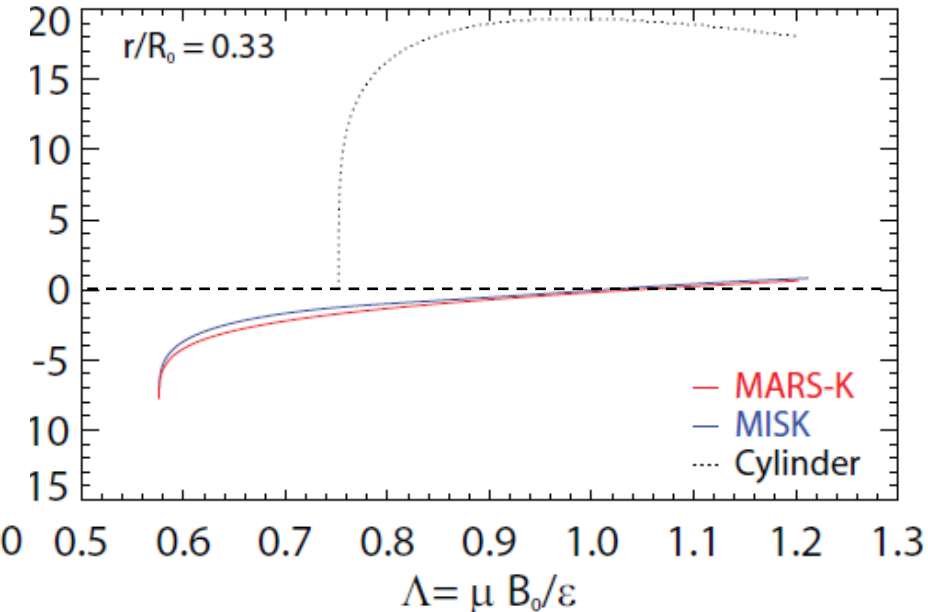
[Jucker et al.,  
Phys. Plasmas 15,  
112503 (2008)]

# Significant issue resolved: The precession drift frequencies now agree

Solov'ev case 1 (near-circular)



Solov'ev case 3 (shaped)



- Metric coefficients corrected in PEST interface to MISK

$$\omega_D = -\frac{1}{\tau} \int \frac{1}{v_{\parallel}} \mathbf{v}_D \cdot (\nabla \phi - \hat{q} \nabla \theta) d\ell - \frac{1}{\tau} \int_{\theta(t)}^{\theta(t')} \hat{q} d\theta.$$

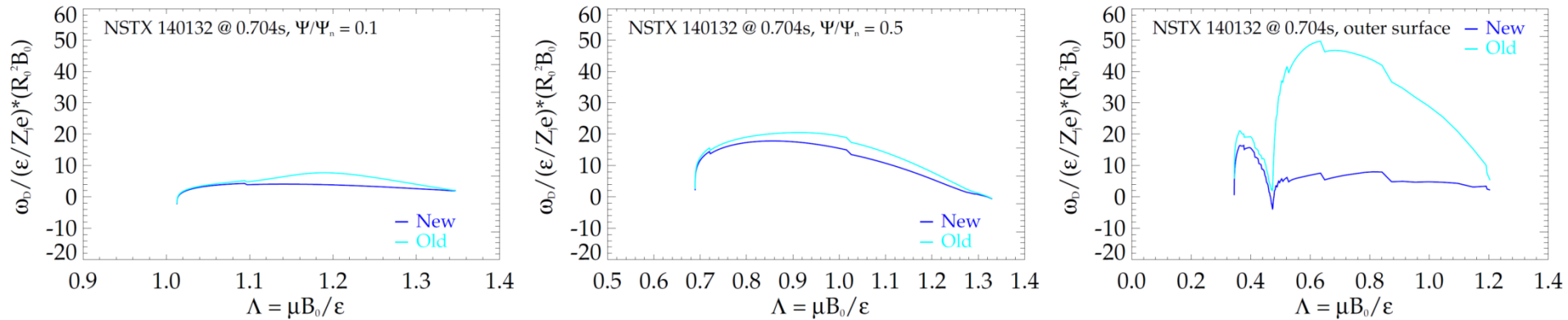
if  $\Psi$  and  $\theta$  are orthogonal:

$$\hat{q} \mathbf{B} \times \nabla \theta = \frac{(\mathbf{B}_{\phi} \cdot \nabla \phi) (\mathbf{B}_{\phi} \times \nabla \theta)}{\mathbf{B}_{\theta} \cdot \nabla \theta}$$

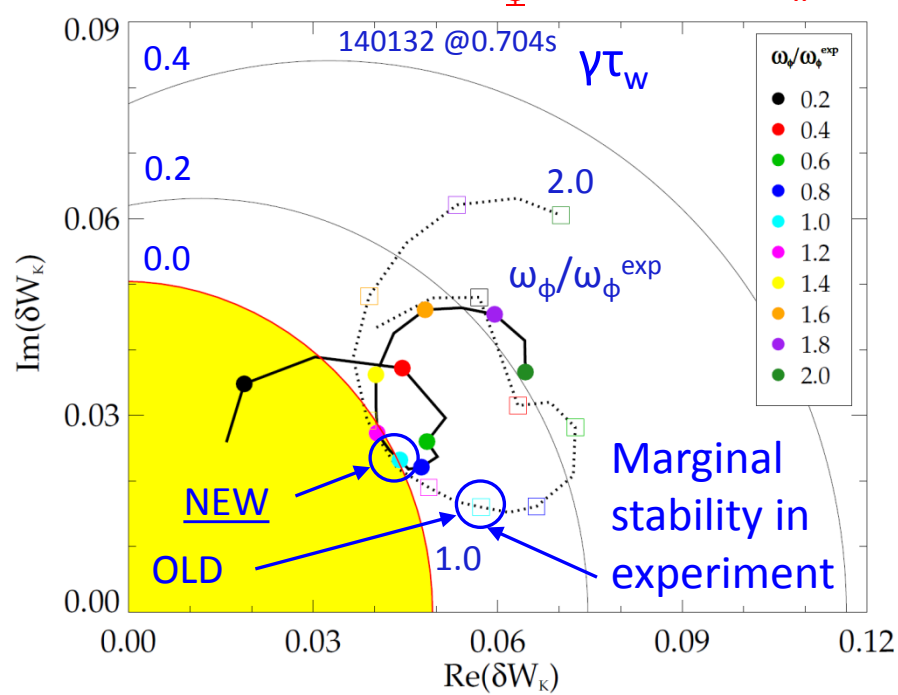
But in PEST,  $\Psi$  and  $\theta$  are non-orthogonal:

$$\hat{q} \mathbf{B} \times \nabla \theta = \frac{\mathbf{B}_{\phi} \cdot \nabla \phi}{(\mathbf{B}_{\phi} \cdot \nabla \theta + \mathbf{B}_{\theta} \cdot \nabla \theta)} (\mathbf{B}_{\phi} \times \nabla \theta + \mathbf{B}_{\theta} \times \nabla \theta)$$

# How does $\omega_D$ correction effect NSTX results? Mostly affects outer surfaces; characteristic change of $\gamma\tau_w$ with $\omega_\phi$ is the same.



RWM stability vs.  $\omega_\phi$  (contours of  $\gamma\tau_w$ )



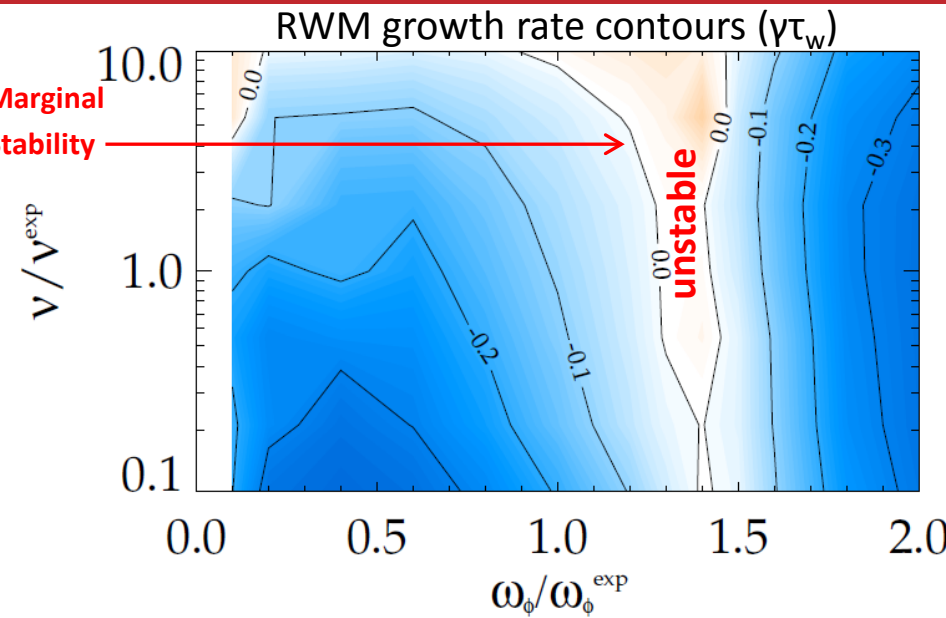
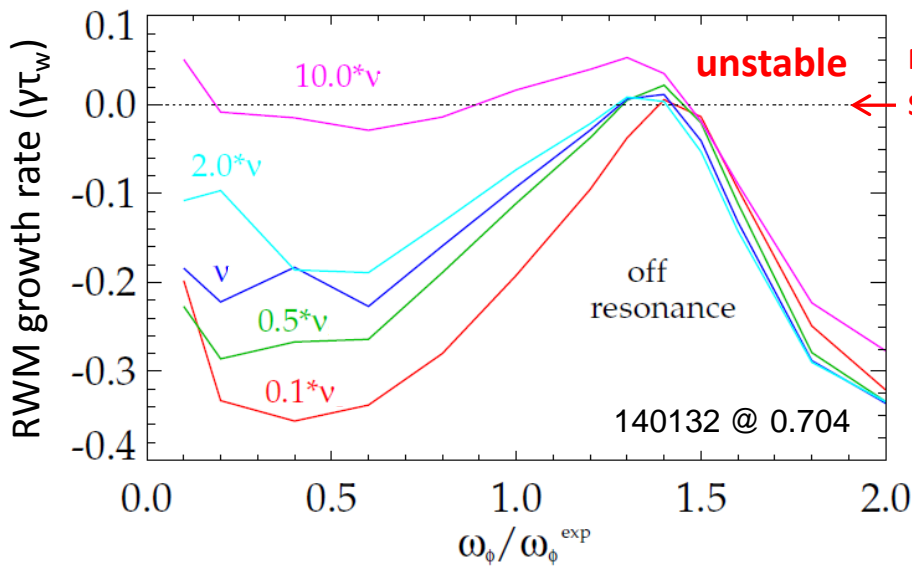
- Affects magnitude of  $\delta W_K$ , but not trends
- In this case, agreement with the experimental marginal point improves
  - Calculations continue to determine the effect of the correction on wider range of cases

# Benchmarking process is now at the point of determining agreement in components of stability computations

Work in progress!

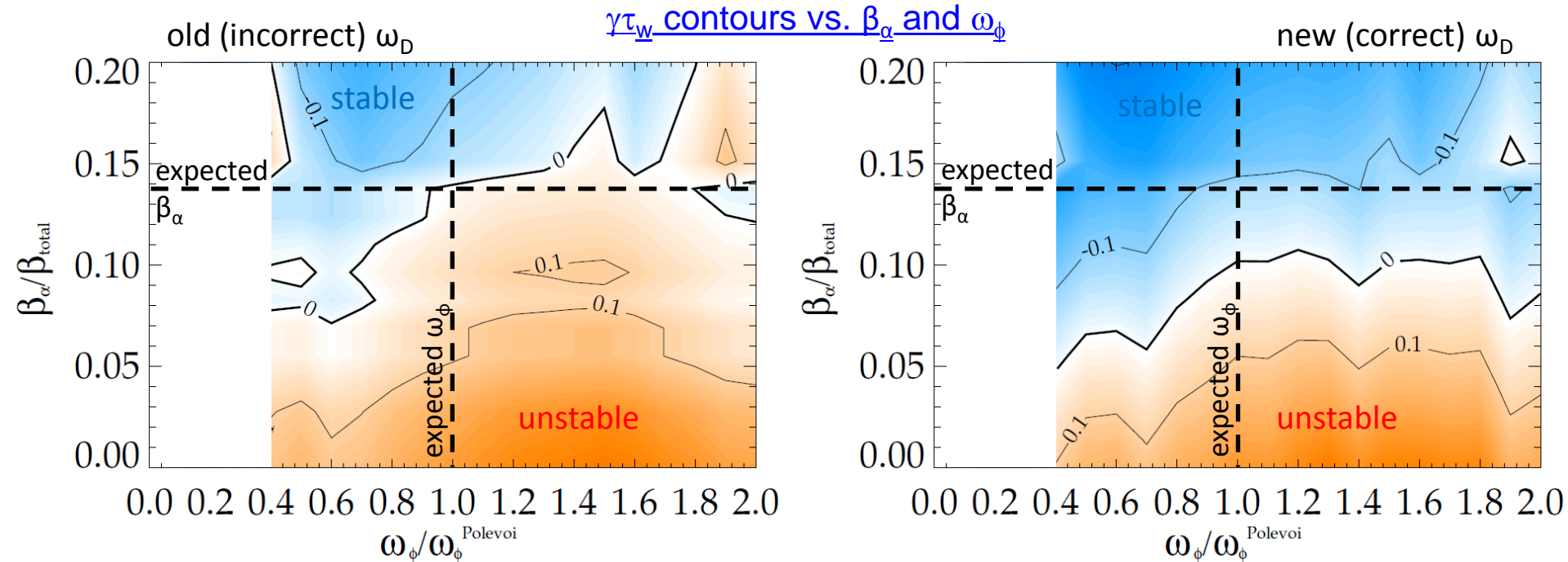
	$r_{\text{wall}}/a$	Ideal $\delta W$ /(- $\delta W_{\infty}$ )	$\text{Re}(\delta W_K)$ /(- $\delta W_{\infty}$ )	$\text{Im}(\delta W_K)$ /(- $\delta W_{\infty}$ )	$\gamma\tau_{\text{wall}}$	$\omega\tau_{\text{wall}}$
<u>Solov'ev 1</u> (MARS-K) (MISK)	1.15	1.187 1.122	0.0256 0.0243	-0.0121 0.0280	0.804 0.850	-0.0180 -0.0452
<u>Solov'ev 3</u> (MARS-K) (MISK)	1.10	1.830 2.337	0.208 0.371	-0.343 0.060	0.350 0.232	-0.228 -0.027
<u>ITER</u> (MARS-K) (MISK)	1.50	0.682 0.677	141.5 0.665	2.286 -0.548	-0.988 0.071	0.00019 0.437

- Calculations from MISK, and MARS-K (perturbative)
  - Good agreement on ideal  $\delta W$ , Solov'ev 1  $\text{Re}(\delta W_K)$ ,  $\gamma\tau_{\text{wall}}$
  - Less agreement on Solov'ev 3
  - Very different ITER result



- NSTX-tested kinetic RWM stability theory: 2 competing effects at lower  $v$ 
  - Stabilizing collisional dissipation reduced (expected from early theory)
  - Stabilizing resonant kinetic effects enhanced (contrasts early RWM theory)
- Expectations in NSTX-U, tokamaks at lower  $v$  (ITER)
  - Stronger stabilization near  $\omega_\phi$  resonances; almost no effect off-resonance
  - Plasma stability gradient with rotation increases
    - important to avoid unfavorable rotation, suppress transient RWM with active control

[J. Berkery *et al.*, Phys. Rev. Lett. **106**, 075004 (2011)]



- ITER requires alpha particles for stabilization across all rotation values.
  - Quantitatively different, but generally consistent with previously analyzed case (in: [J.W. Berkery et al., Phys. Plasmas 17, 082504 (2010)])
- Correction to  $\omega_D$  makes calculation more stable, but doesn't affect the general conclusions

# RWM kinetic stability model is being validated by comparison to experiments and is being benchmarked with other codes

- Benchmarking:
  - Early NSTX calculations found some quantitative differences between marginal point and experiment.
  - Improved results, with additional physics (such as EPs) and code improvements, better match experiments.
  - Benchmarking exercise led to correction of  $\omega_D$  calculation.
- Physics implications:
  - Energetic particles needed for quantitative agreement with NSTX; EP distribution matters.
  - Stronger stabilization near  $\omega_\phi$  resonances in low  $v$  devices.
  - Alpha particles required for stability at all  $\omega_\phi$  in ITER.

*Supported by U.S. Department of Energy Contracts: DE-FG02-99ER54524, DE-AC02-09CH11466, and DE-FG02-93ER54215*

**XXX**

---

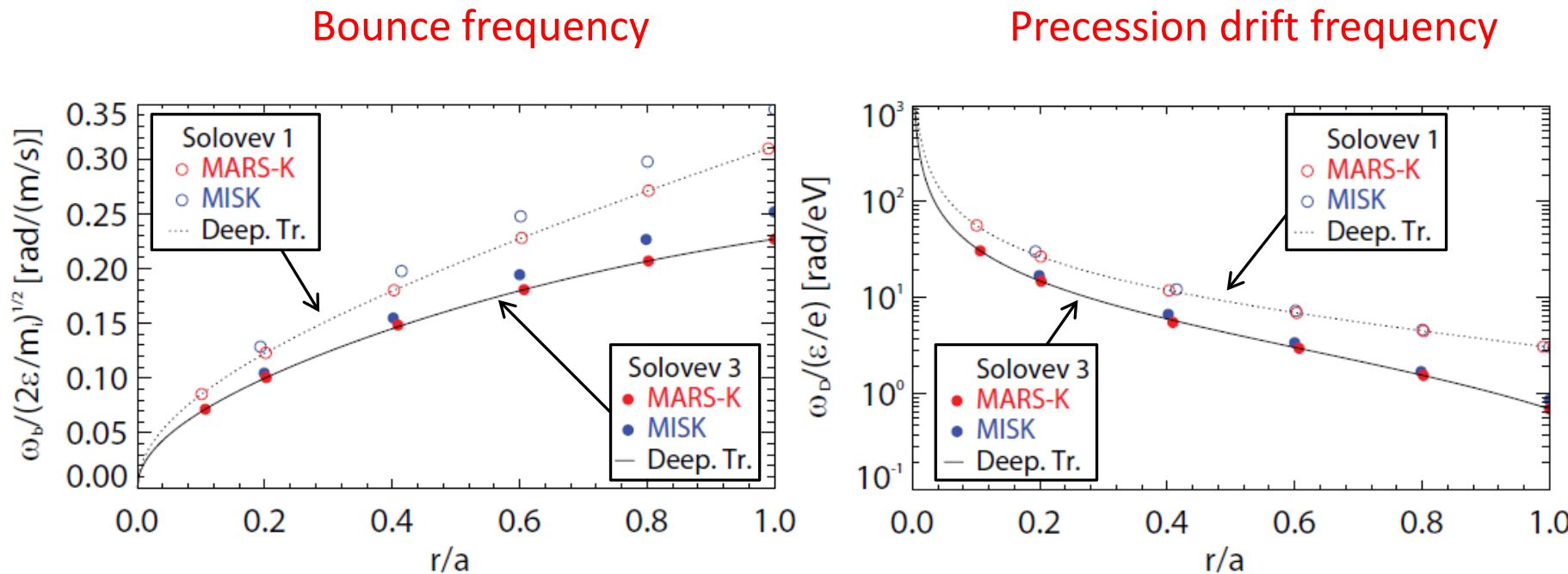
# Benchmarking process is now at the point of determining agreement in components of stability computations

Work in progress!

	$r_{\text{wall}}/a$	Ideal $\delta W$ /(- $\delta W_{\infty}$ )	$\text{Re}(\delta W_K)$ /(- $\delta W_{\infty}$ )	$\text{Im}(\delta W_K)$ /(- $\delta W_{\infty}$ )	$\gamma \tau_{\text{wall}}$
<u>Solov'ev 1</u> (MARS-K) (MISK)	1.15	1.187 1.122	0.0256 0.0243	-0.0121 0.0280	0.804 0.850
<u>Solov'ev 3</u> (MARS-K) (MISK)	1.10	1.830 2.337	0.208 0.371	-0.343 0.060	0.350 0.232

- Calculations from MISK, and MARS-K (perturbative)
  - Good agreement on ideal  $\delta W$ , Solov'ev 1  $\text{Re}(\delta W_K)$ ,  $\gamma \tau_{\text{wall}}$
  - Less agreement on Solov'ev 3
  - Different  $\text{Im}(\delta W_K)$  – may have a simple explanation

# Bounce and precession drift frequency radial profiles agree (deeply trapped regime shown)



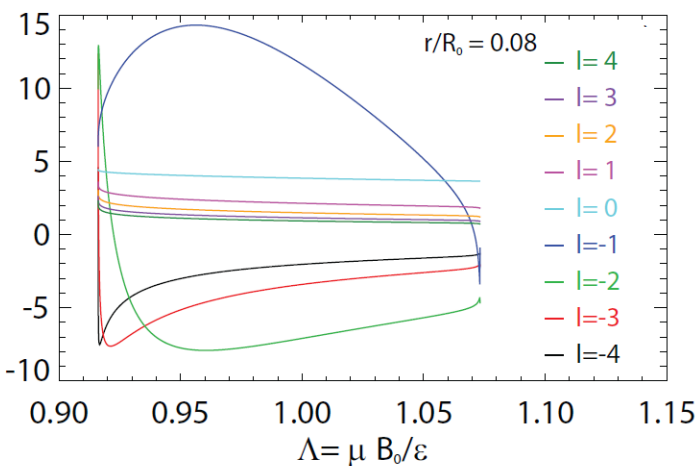
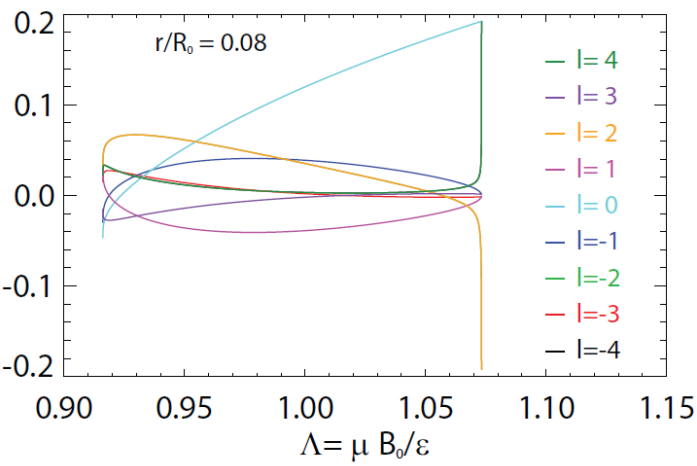
Deeply trapped limit

$$\frac{\omega_b}{\sqrt{2\epsilon/m_i}} = \frac{1}{q_0} \left( \frac{F^2}{1+2\epsilon_r} + \frac{\kappa^2 \epsilon_r^2}{q_0^2} \right)^{-1} \left[ \frac{F^2 \epsilon_r}{2(1+2\epsilon_r)} + \frac{\kappa^2 \epsilon_r^3}{q_0^2} + \frac{(1-\kappa^2) \epsilon_r^2}{2q_0^2} (1+2\epsilon_r) \right]^{\frac{1}{2}}$$

- Good agreement across entire radial profile

# The kinetic term can be split into two pieces that depend on the eigenfunction or the frequencies, for code comparison

Solov'ev case 1 (near-circular)



$$\delta W_K = -\frac{\sqrt{\pi}}{2} \int_0^{\Psi_a} \frac{nT}{B_0} \int_{B_0/B_{\max}}^{B_0/B_{\min}} \tau \sum_l \langle H/\hat{\varepsilon} \rangle^2 I_{\hat{\varepsilon}} d\Lambda d\Psi.$$

Perturbed Lagrangian

$$\langle H/\hat{\varepsilon} \rangle (\Psi, \Lambda, l) = \frac{1}{\tau} \oint \frac{1}{\sqrt{1 - \frac{\Lambda B}{B_0}}} \left[ \left( 2 - 3 \frac{\Lambda B}{B_0} \right) (\boldsymbol{\kappa} \cdot \boldsymbol{\xi}_{\perp}) - \left( \frac{\Lambda B}{B_0} \right) (\nabla \cdot \boldsymbol{\xi}_{\perp}) \right] e^{-il\omega_b t} d\ell.$$

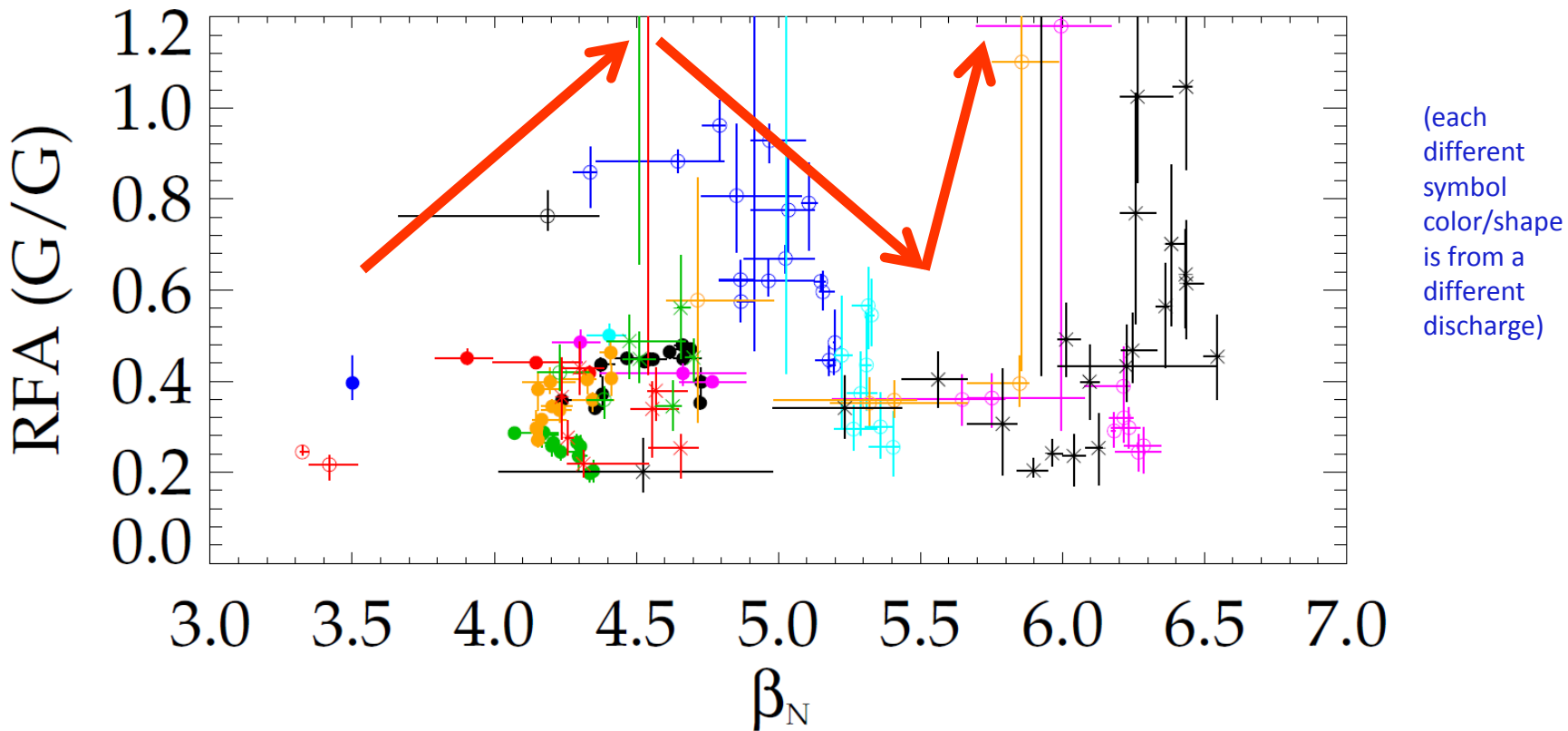
- Depends mostly on the eigenfunction.

Energy integral of the frequency resonance fraction

$$I_{\hat{\varepsilon}} (\Psi, \Lambda, l) = \int_0^{\infty} \frac{\omega_{*N} + \left( \hat{\varepsilon} - \frac{3}{2} \right) \omega_{*T} + \omega_E - \omega_r - i\gamma}{\omega_D + l\omega_b + \omega_E - i\nu_{\text{eff}} - \omega_r - i\gamma} \hat{\varepsilon}^{\frac{5}{2}} e^{-\hat{\varepsilon}} d\hat{\varepsilon}.$$

- Does not depend on eigenfunction, just frequency profiles

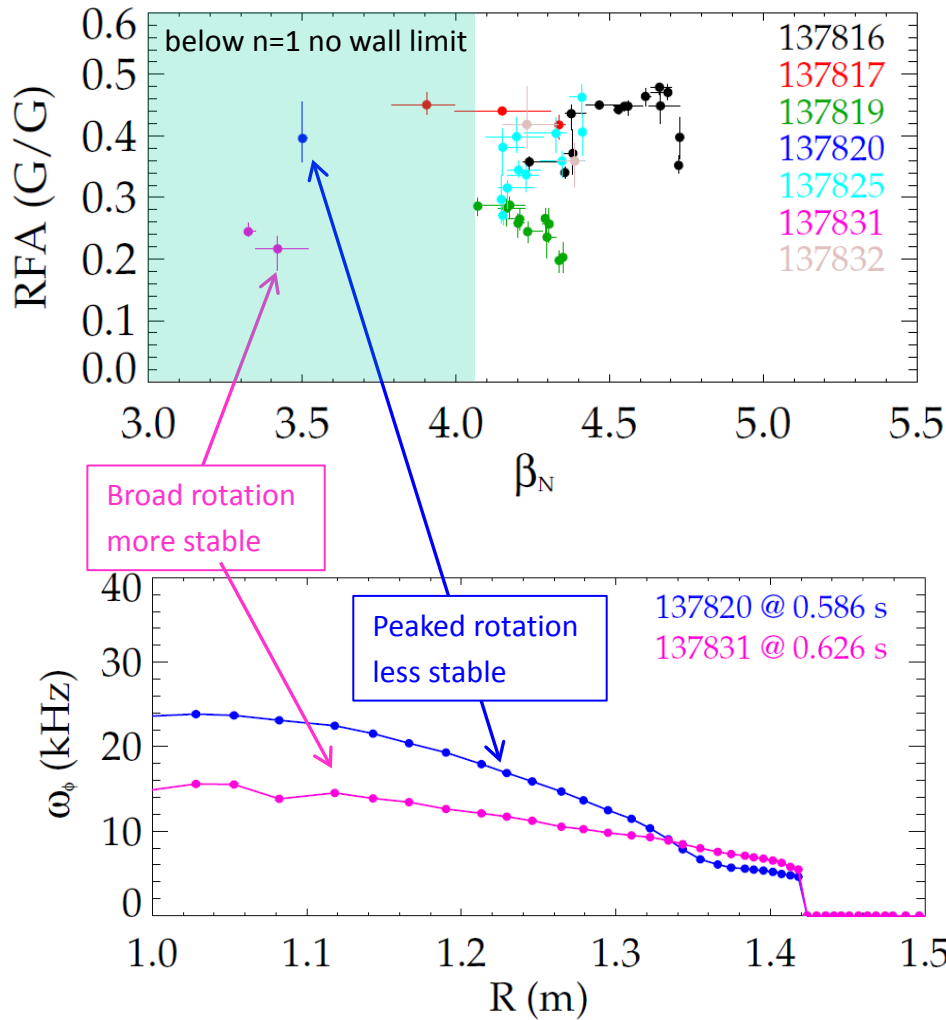
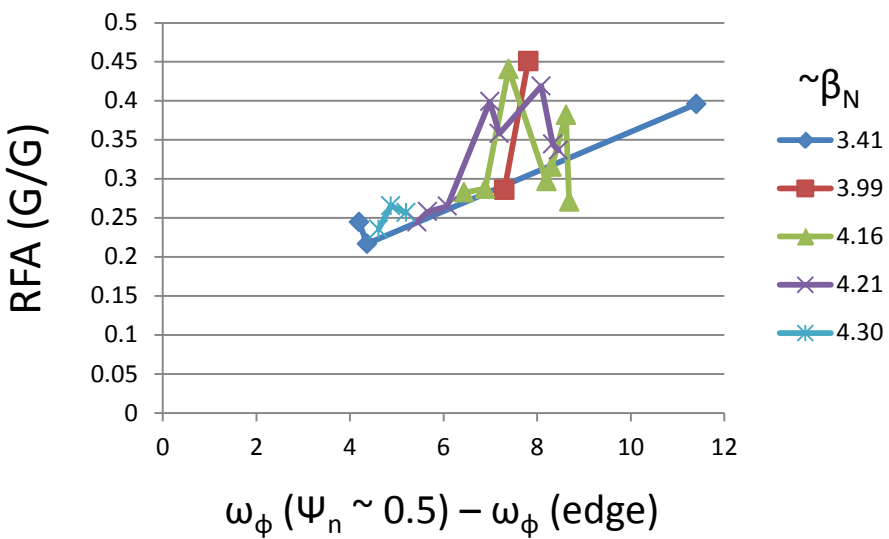
# Latest NSTX experiments: Maximum RFA amplitude does not monotonically increase with increasing $\beta_N$



- Examine resonant field amplification (RFA) amplitude to determine proximity to the marginal point
  - shows increased stability at intermediate  $\beta_N$  ( $\sim 5.2 - 5.8$ ).
- In other machines (DIII-D, JET) RFA increases with  $\beta_N$

# RFA response is greater with more peaked $\omega_\phi$ , at lower $\beta_N$

- RFA response observed below  $n = 1$  no-wall  $\beta$  limit
  - Common in tokamaks
- RFA increases with rotation gradient at  $\sim$  constant  $\beta_N$ .



# Above the no-wall limit, RWM stability dependence on $\omega_\phi$ profiles is complex

- More specifically, RWM stability / RFA depends on energy dissipation due to kinetic resonances
  - Depends on  $\omega_\phi$  profile.
  - Sensitivity to rotation in the outer surfaces where the RWM  $\xi$  is large
- Alteration of amplitude and time history of applied  $n = 3$  field creates  $\omega_\phi$  profile variation
- Further characterization of the approach to RWM marginal stability is underway

